Artificial Magnetic Conductor Based Miniaturized Frequency Re-configurable Dielectric Resonator Antenna for 5G and WBAN Applications

Shahid Khan [1], Hazrat Ali [2], Syed Usman Ali Shah [2], Haider Ali [3], and Camel Tanougast [1]

[1] Institut Supérieur d'Électronique et d'Automatique
University De Lorraine, Metz, Lorraine, 57070, France

[2] Department of Electrical and Computer Engineering
COMSATS University Islamabad, Abbottabad, 22060, Pakistan

[3] Department of Electronics Technology, University of Technology, Nowshera, Pakistan
shahid.khan@univ-lorraine.fr, hazratali@cuiatd.edu.pk, syedusman.eng@gmail.com,
haider.ali@uotnowshera.edu.pk, camel.tanougast@univ-lorraine.fr

Abstract ─ In this work a novel miniaturized frequency reconfigurable Dielectric Resonator antenna using Artificial Magnetic Conductor (AMC) surface is proposed. The prototype is set to work for 5G mid-band frequencies and Wireless Body Area Network (WBAN) applications. The work consists of two parts: firstly, the miniaturization of the prototype using AMC surface and secondly using the same AMC surface to reconfigure the frequency to another wireless application. Using AMC surface, the DR volume is reduced by 85% percent. Connecting the AMC unit cells through ideal switches (micro-trip slabs) re-configures the DR for different frequency. The overall performance observed before switching as well as after switching in both the cases is promising. The design is fabricated for performance analysis. A close agreement is reported between simulated and measured values of the reflection coefficients, radiation pattern, gain and efficiencies. The prototype has stable radiation pattern for both the operating frequencies. The impedance bandwidth values for both the resonance frequencies are 14.2% and 16% respectively. The prototypehas a maximum gain of 6.8dBi and a maximum efficiency of 88%.

Index Terms ─ 5G, artificial magnetic conductor, dielectric resonator antenna, efficiency, gain, WBAN.

I. INTRODUCTION

Modern communication systems are rapidly evolving. They tend to offer a number of services to the end users without compromising the device compactness. To keep the volume of the device compact, different blocks of the communication systems need to be carefully designed. One important block is the front end including the antenna. Due to limited space availability for the antenna in any communication system, antennas need to be designed carefully so that it may be accommodated

easily with the provision of multiple wireless services.

3-D View of the design
(a)

Back View
(b)
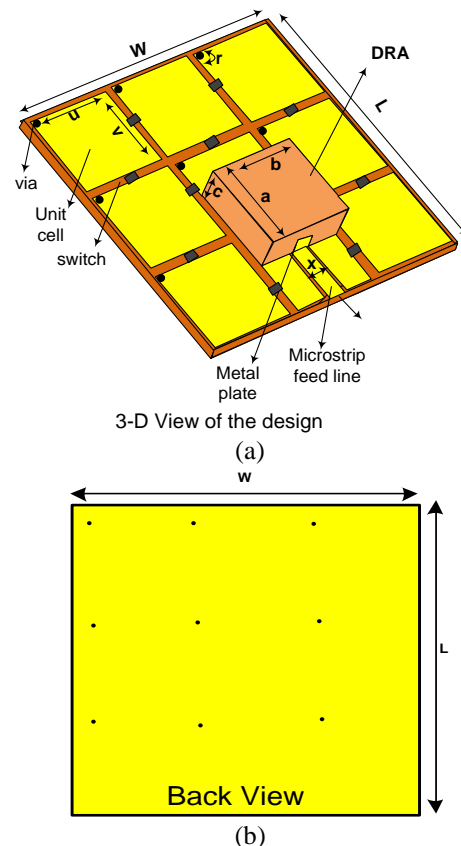
Fig. 1. (a) Represents 3-D front view, and (b) represents the back side of the design.

A number of antenna designs have been proposed for size miniaturization and frequency re-configurability by using different techniques. However, there are very

few published works which focus simultaneously on both these aspects by using AMC surface. Traditionally, the AMC surface has been in use for different wireless applications. It can be used to excite additional frequencies for different wireless applications [1]. In [2], a low profile circularly polarized meta-surface based antenna is presented, where the meta-surface is used as an independent radiator. In [3], AMC surface is used to enhance the bandwidth of the low profile antenna. Thus, AMC surface enhances the bandwidth, the reflection co-efficient and gain of the antenna. In [4], a compact low profile meta-surface based antenna for medical application is proposed. In this work, addition of the AMC surface with the antenna not only enhances the overall performance of the design but also reduces the specific absorption rate by 95.3%.

Along with the other applications, AMC surface is also useful for the re-configurability of different antenna parameters. With the help of AMC surface, we can perform frequency re-configurability, pattern re-configurability, waveform re-configurability and beam steering. In [5]-[6], AMC surface is used to control re-configurability independently. The active switches and varactor diodes are inserted in the AMC surface [7]. This not only helps to maintain the performance of the design but also performs re-configurability for certain parameters. In all the mentioned examples, the micro-strip patch antennas (MPA) accompany AMC surface. Despite of generating some good results, MPAs have still some shortcomings like narrow bandwidth, low gain, low efficiencies and unstable radiation pattern thus they have enough room for improvement in the overall performance parameters. DRA in combination with the AMC surface can provide good performance parameters like wider bandwidth, stable radiation pattern with good values of gain and efficiencies, as both these independent structures have characteristics of generating good performance results. Therefore, DR can be a good candidate and replacement of MPAs for different wireless applications [8]. However, the DRs have relatively larger size (volume). In the literature very few miniaturized frequency reconfigurable DRAs have been reported. In [9]-[10], different compact and miniaturized DRAs have been reported. In all these examples, the prototypes are either miniaturized or reconfigured separately. There are very few examples, which jointly focus on both the miniaturization and re-configurability aspects. To the best of our knowledge, no work has been reported to miniaturize and re-configure DRAs simultaneously with the help of AMC surface.

In this work, we present a novel re-configurable miniaturized DRA with the help of AMC surface. The AMC surface miniaturizes and re-configures the prototype with overall good performance parameters. The prototype is miniaturized by 85% and re-configured between two operating frequencies for 5G mid-band frequencies and WBAN applications respectively.

II. THEORITICAL BACKGROUND

For the design of the proposed work, the first step is to design DR. For this purpose, a rectangular DR is selected, as it is easy to fabricate and gives more degree of dimension freedom. The initial size of the DR for the 5G mid-band frequency application is designed with the help of the following Dielectric Waveguide model (DWM) [8]-[13]:

$$f_r = \frac{C}{2\pi\sqrt{\in_r}}\sqrt{K_x^2 + K_y^2 + K_z^2}$$
$$K_x = \frac{\pi}{a} \; ; \quad K_z = \frac{\pi}{c} \quad\quad (1)$$
$$K_y \tan\left(K_y \frac{b}{2}\right) = \sqrt{(\in_r - 1)\left(K_0^2 - K_y^2\right)}.$$

The three dimensions of the DR calculated with the help of equation (1) are a, b and c while K_x, K_y, and K_z are the wave numbers across the three sides of the DR. C is the speed of light in free space.

The initial size of the DR gives the target resonance frequency, but the design has a large volume. To address this issue, AMC surface is used. Importantly, each single unit of AMC surface must also have the same resonance frequency. To do this, the AMC surface is carefully designed with the help of following equations [7]:

$$f_r = \frac{1}{2\pi\sqrt{LC}}. \quad\quad (2)$$

Equation (2) defines the resonance frequency of the AMC unit cell. This resonance frequency is dependent on the capacitive and inductive reactance of the AMC surface. The inductance is offered by the metallic vias between the AMC unit cells and ground while capacitances are offered by the gap between the AMC unit cells. To design the AMC unit cells for 3.5GHz resonance frequency, the following equations are incorporated:

$$C = \frac{W\varepsilon_0(1+\in_r)}{\pi} \cosh^{-1}(\frac{w+g}{g}), \quad\quad (3)$$

$$L = 2 \times 10^{-7}h\left[\ln\left(\frac{2h}{r}\right) + 0.5\left(\frac{2r}{h}\right) - 0.75\right]. \quad\quad (4)$$

Where, $w = 0.18\lambda_{3.5ghz}$, $g = 0.01\lambda_{3.5ghz}$, and $r = 0.005\lambda_{3.5ghz}$.

The values obtained from Eqs. (3) and (4) are then placed in Eq. (2). The calculations give resonance frequency value in accordance to what we obtain from the DRA. The total number of AMC unit cells are decided from the resonance frequency shift to the same value of the un-miniaturized DRA. Once DR is positioned on the 3×3 arrangement of the AMC unit cells, the current distribution from the AMC surface couples the current distribution inside the DR, thus both the structures resonate at 3.5GHz. Thus, net result is the combined effect of both the structures.

III. ANTENNA DESIGN DISCUSSION

The proposed simple design consists of DR with low permittivity ($\mathbf{\varepsilon_r = 10}$) positioned on FR4 substrate with 1.6mm thickness and 0.002 tangent loss. Both the length and the width of the ground substrate and ground metal

are equal to 60mm. Initially, the DR dimensions are determined by using DWM (Dielectric Waveguide Model) [11]. The three dimensions **a, b,** and **c** are length, width and height of the proposed prototype, which are 20mm, 21mm, 10mm respectively. After determining the initial dimensions of the DR. The DR is fed by a micro-strip line of 3mm width and has a gap of 0.1mm with the neighboring AMC unit cells. A micro-strip patch which is the extended feedline is stacked to the wall of the DR to improve the impedance matching. The design with the initial volume of 4200mm^3 resonates at 3.5GHz. In the next step the volume of the DR is reduced to 605mm^3 by using AMC surface. Figures 1 (a) and (b) explains the top and bottom view of the design in detail. Table 1 represents details of the different dimensions of the proposed design.

A unit cell of the AMC surface was carefully designed at 3.5GHz. The unit cell has a high impedance surface (HIS) characteristic at 3.5GHz. When these AMC unit cells are positioned together, they are then connected to the ground plane with the help of thin metallic vias of 0.4mm radius. Closely analyzing the prototype, it is observed that an RLC resonance circuit is developed. The gap between AMC unit cells introduce capacitances and metallic vias generate inductive effects. Thus the combination of 9 unit cells resonate at 3.5GHz. When the volume of independent DR is reduced to 650mm^3, the frequency moves to 4.3GHz because resonance frequency has an inverse relationship with size of the DR. A decrease in the volume of the DR will shift the resonance frequency of the DR to higher value and vice versa. After doing this, the reduced DR is placed above the array of nine unit cells. As AMC surface act as an independent resonance structure, when the reduced DR couples with AMC surface they both resonate in a single frequency. Due to its metallic nature, the bandwidth is slightly reduced because of the relatively narrow bandwidth response of the AMC surface. In the next phase re-configurability was managed with the help of ideal switches positioned between the AMC cells. These switches are small micro-strip patches of 1×1mm^2. Placement of the ideal switches reduces the capacitance between the AMC unit cells as shown in (2). Reduction of the capacitance between the AMC unit cells causes the shift of resonance frequency to higher frequency thus it resonate the design at 4.2GHz. At both the resonance frequencies the design has stable radiation pattern with the good values of the gain and efficiencies.

During the simulation, the switching circuit was performed with the help of PIN diode, resistors, capacitors and inductors. The equivalent schematic of this switching circuitry was also analysed and both showed great resemblance in terms of simulated results RF PIN diodes BAR 50-02V switch OFF and switch ON the circuit while resistor of 100 Ω limit the current flow to protect the circuit elements and similarly the presence

of micro-strip slabs show ON state and their absence show OFF state. The capacitor of 22Pf during the simulation block the flow of DC into input RF port while inductor of 100 pH block the flow of AC current into DC biasing circuit. The above mentioned biasing circuitry during the simulation performs the switching operations. Looking to the close resemblance between the two switching schemes, micro-strip slabs were selected as final switching option as they are easy to simulate and fabricate. There are two switching categories i-e, OFF state and ON state. A total of 12 switches in the form of small micro-strip patches are used for frequency re-configurability. Absence of all the switches makes configuration I (OFF state) and presence of all the switches makes configuration II (ON state). At configuration I antenna resonate at 3.5GHz and at configuration II the prototype is reconfigured to 4.2GHz.

Table 1: Different parameters of the design

Parameters	Without EBG	With EBG
$L_g \times W_g \times H_s$	$(60 \times 60 \times 1.6)$ mm^3	$(50 \times 50 \times 1.6)$mm^3
$a \times b \times c$	$(20 \times 20 \times 12)$ mm^3	$(10 \times 10 \times 5)$ mm^3
$u \times v$	-	(15.17×15.7)mm^2
g	-	0.75mm
r	-	0.404mm
L_f	10mm	10mm
W_x	3mm	3.0mm

IV. PARAMETRIC STUDIES

In order to finalize the design for both the miniaturization and re-configurability a number of optimization techniques for different parameters are performed. It includes the effect of attached micro-strip patch to the wall of DR, which is actually the extended feed line. Another important parameter for optimization is the effect of AMC unit cell area on the resonance frequencies. The effect of the number of AMC unit cells on the resonance frequencies are also observed. Lastly, the effect of switches and location of the switches on the frequency re-configurability is also studied.

The extended feedline to the wall of the DR highly effect the impedance matching. Figure 2 shows that as we increase the height of the stacked micro-strip line, the impedance matching improves and a slight increase in the bandwidth is observed because of change in current distribution inside the DR. Thus, maximum matching and relatively wider bandwidth is achieved at 5.22mm height of the extended feedline.

Area of the unit cell also highly affects the resonance frequency. Any increase or decrease in the AMC unit cell area change the high impedance surface (HIS) characteristics, which shifts the resonance frequency. Figure 3 shows that increasing the area of the unit cells shifts the frequency to lower range and vice versa.

It is also clear from the Fig. 3 that an area

of (15.17mm×15.7 mm) gives the required resonance frequency with much better impedance matching. Figure 3 also shows that an increase in the unit cell area has an inverse relationship with the resonance frequency.
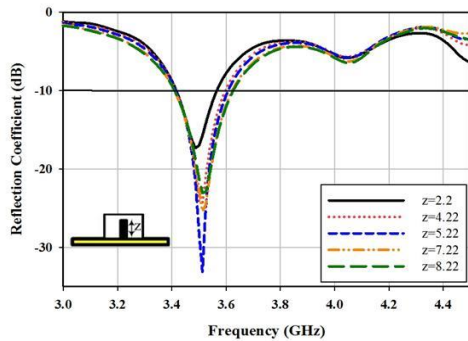
Fig. 2. Effect of the feedline extension.
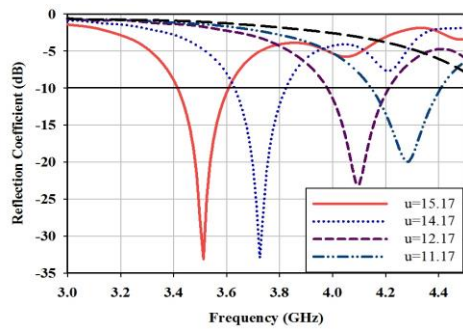
Fig. 3. Effect of AMC unit cell area on S11.
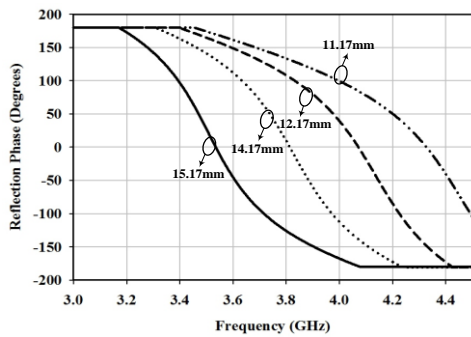
Fig. 4. Phase angle diagram of the Unit Cell.

The phase angle diagram shows that zero crossing of the unit cell has an inverse relationship with the area of the AMC unit cell. Figure 4 shows the effect of changing unit area on the zero crossing of the resonance frequency. Increasing the area of the unit AMC cell causes the shift in zero crossing to low range frequencies and vice versa. (15.17×15.7 mm^2) is the final area of the unit cell at 3.5GHz. Similarly, the number of AMC unit

cells also affects the resonance frequency. As AMC surface can act as an independent resonance structure so the number of unit cells can increase or decrease the resonance frequency.

Introduction and location of the switches has also a significant impact on the resonance frequencies. Figure 5 shows the effect of location of switches on the resonance frequencies. The location of the switches were tested on three different points. From Fig. 5, it is clear that with no switches the antenna resonates at 3.5GHz. When the switches are positioned at the top edge of the AMC unit cells, the resonance frequency shifts to higher range but still the required resonance frequency is not achieved. The switches are then tested at bottom position. The location of the switches at this position further shift the resonance frequency but the required resonance frequency is still missing. In order to achieve the required resonance frequency the switches are positioned at the midpoint of the unit cell. From Fig. 5, it is clear that at this position, the antenna resonates at 4.2GHz, which is the required resonance frequency. The final location selected for the position of the switches is the mid-point of the AMC unit cell, which resonates the design at 4.2GHz. The possible reason for the shifting of the resonance frequency to higher frequency is the changing values of the capacitances between the unit cells. It is clear that there is a small gap between the unit cells. This gap actually introduces the capacitances in the overall design. Any change in the capacitance changes the resonance frequency. Introduction of the switches reduces the overall capacitances and thus frequency shift to higher range. The maximum decrease in the equivalent capacitance is observed when switches are positioned at mid of the AMC unit cell. During the simulation process, the switching was performed with the help of micro-strip slabs (ideal switches). In the fabrication of the prototype, they are replaced with a micro-strip line of 1×1mm^2.
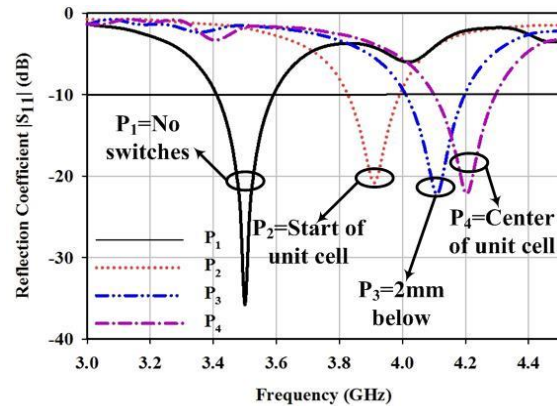
Fig. 5. Effect of location of switches at different positions.

V. RESULTS AND DISCUSSION

In this section different simulated and measured results of the proposed design are discussed in detail. These results include simulated results before and after miniaturization. It also includes simulated and measured values of the reflection coefficients of the prototype before and after frequency re-configurability. Simulated and measured radiation pattern is also explained in detail. Similarly simulated and measured efficiency and gain for both the configurations have also been presented in detail.

In Fig. 6 it is seen that an un-miniaturized DR resonates at 3.5GHz with a wider bandwidth. When its size is directly reduced without using AMC unit cells the resonance frequency shifts to higher range and it resonates at 4.8GHz because size of the DR has an inverse relationship with the resonance frequency. Figure 6 also shows that addition of AMC unit cells shifts back the resonance frequency and resonate the design at 3.5GHz. AMC unit cells are independent resonant structures which resonate at a specific resonance frequency. When AMC surface is coupled with the DR they support each other but the bandwidth is slightly reduced because net bandwidth is the combined effect of both the structures. AMC surface has slightly narrow bandwidth response (because of metallic nature) and DR has a wider bandwidth response after combining them with each other, the net result is slight reduction in the bandwidth.
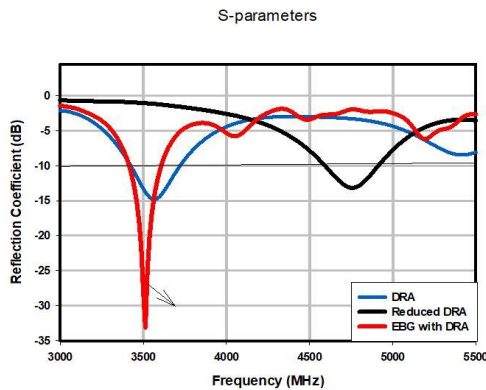
Fig. 6. Reflection coefficient of DRA before and after miniaturization.

The application of the AMC surface greatly reduced the DR size. The next step was to reconfigure the frequency by using the same AMC surface. Using the effect of changing equivalent capacitance after adding small micro-strip patches helped to reconfigure the frequency to WBAN wireless application. Switches in the form of small micro-strip patches are introduced in

between the AMC unit cells which shifts the frequency to high range. Figure 7 shows that absence of the small micro-strip patches (switches) which represents OFF state resonates the design at 3.5GHz. The simulated and measured values are in close agreement. The simulated bandwidth is 200MHz and measured bandwidth is 180MHz. There is minor shift in the resonance frequency and also a reduction in the bandwidth. The shift in the resonance and reduction of the bandwidth is because of the fabrication inaccuracies. Provision of fine fabrication can overcome this problem.

Figure 8 shows the reconfigured prototype frequency when all switches are ON. When switches are positioned at the mid of the AMC unit cells, frequency is reconfigured to 4.2GHz for WBAN application. Simulated bandwidth is 200MHz and measured bandwidth is 230MHz. Simulated and measured resonance values are close enough with a slight difference in the bandwidth because of intolerances due to fabrication. A good and more accurate fabrication can overcome this problem.
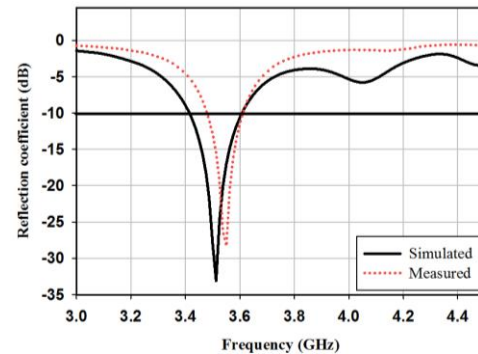
Fig. 7. Simulated and measured reflection coefficient in OFF state.
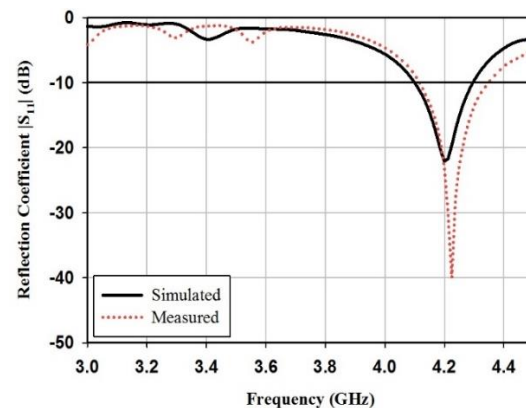
Fig. 8. Simulated and measured reflection coefficient in ON state.

Table 2: Comparison of the current work with already published work

No.	Antenna Type	DR Volume	Re-configurability	Design Complexity	Gain	Efficiencies	% Bandwidth
1	Compact RDRA [10]	0.12λ×0.17λ×0.5 λ	Reconfigurable	Simple	5.8dBi	N/A	8%, 16% and 65%
2	Compact RDRA [12]	0.13λ×0.41 λ×0.06 λ	reconfigurable	Simple	N/A	N/A	85% and 14%
3	RDRA with tunnel [11]	0.13λ×0.13 λ×0.27 λ	reconfigurable	Complex	5.0dBi	N/A	60% and 50%
This work	RDRA	0.12λ×0.12λ×0.058 λ	Reconfigurable	Very simple	6.87dBi	88%	14.2%, 16%

Table 3: Performance analysis of the overall design

Switching State	Simulated Bandwidth	Measured Bandwidth	Simulated Efficiencies	Measured Efficiencies	Simulated Gain	Measured Gain
OFF	3.4-3.6 GHz	3.45-3.6 GHz	87%	85%	6.8dBi	6.7dBi
ON	4.1-4.3 GHz	4.13-4.37 GHz	76%	74%	6dBi	5.8dBi
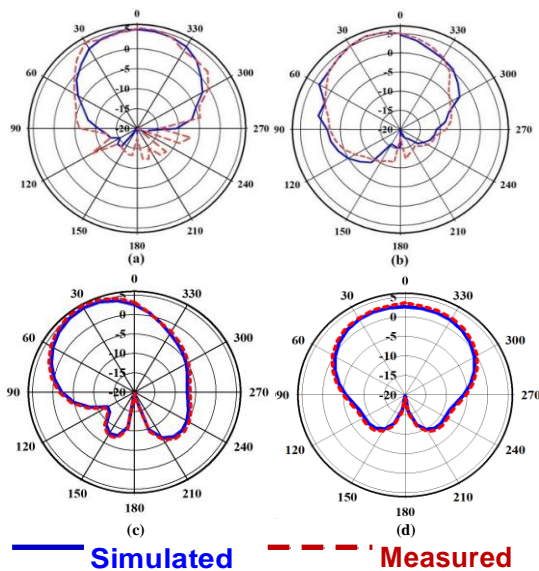
Fig. 9. (a) and (b) show the Simulated and measured E-field and H-field in OFF state, respectively. Similarly, (c) and (d) show simulated and measured E-field and H-field when switches are in ON state, respectively.

Figure 9 shows the simulated and measured radiation pattern for both the switching configurations. The far field radiation pattern is presented in the form of the E-field and H-field. Figures 9 (a) and (b) show the radiation patterns of the design when all switches are in OFF state. From Fig. 9, it is quite clear that radiation pattern for both the E-field and H-field is stable and mainly broad side and focused towards 0°. The value of peak gain is 6.87dBi. Moreover, simulated and measured parameters are in close agreement. A minor deviation is due to the lack of accuracies in the prototype fabrication.

Similarly, Figs. 9 (c) and (d) show the radiation pattern when switches are in ON state. The radiation pattern at 4.2GHz is stable, focused towards 0° and is broadside. The simulated and measured values of the radiation pattern are in close matching which shows that measured values follows strictly the simulated values that define the stability of the design. Thus at both the resonance frequencies the simulated and measured radiation pattern is stable with the good values of gain. This also clarify that switching only changes the frequency of the prototype while the radiation pattern is still stable at the same position.
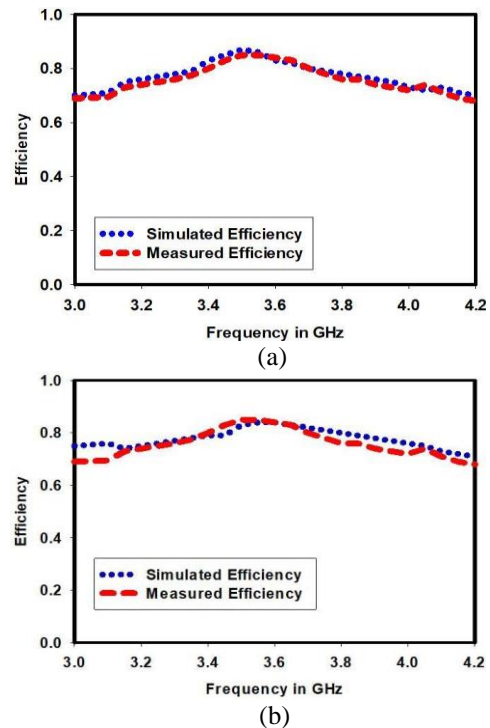
Fig. 10. Efficiencies of the design: (a) when switches are in OFF position, and (b) when switches are in ON position.

In Fig. 10 detailed analysis of the efficiencies for both the arrangements has been presented. In the OFF switching configuration, the simulated efficiency of the design is 87% while measured values of the efficiency is close to the simulated value which is 85%. Similarly in ON switching configuration the efficiency of the design at 4.2GHz is 76% while measured values of the efficiency at the same frequency is 74%. Thus, the simulated and measured values are in close agreement.

Figure 11 shows the simulated and measured values of the gain for both the configurations. For configuration I, the simulated value of the gain is 6.8dBi and measured value is also in very close matching except with a minor deviation at 3.5GHz and 4.2GHz. Similarly, after re-configurability, the simulated value has maintained its value at 6dBi but measured value is slightly less than the simulated one i-e 5.8dBi, however this slight deviation in both the cases is acceptable.

(a)

(b)
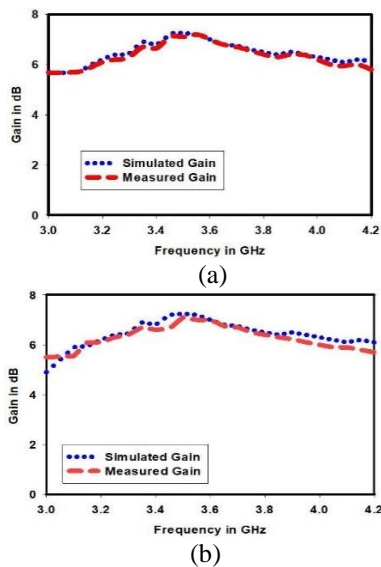
Fig. 11. (a) Gain of the design when switches are in OFF position, and (b) when switches are in ON position.

(a)   (b)
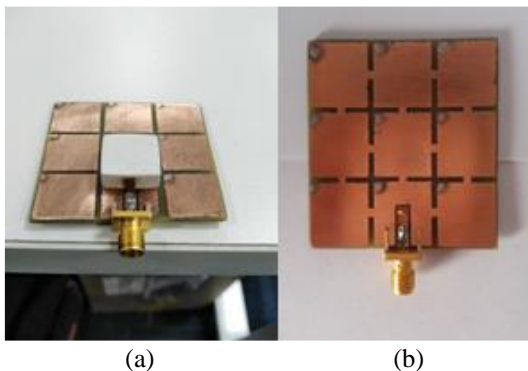
Fig. 12. (a) Represents miniaturized Prototype, and (b) shows the AMC surface with ideal switches.

(a)   (b)
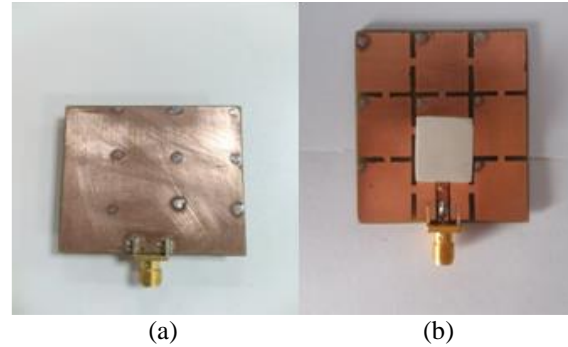
Fig. 13. (a) Rear View of the Prototype, and (b) miniaturized prototype with ideal switches.

In Table 2, a comparison of different published work with the proposed work has been presented. The work in [10] comprises of rectangular DR with relatively smaller volume and simple design. The value of gain is good with two switching operations to achieve three resonance frequencies. The design reported in [12] also represents a compact reconfigurable design with two resonance frequencies. The third design as reported in [11] for re-configurability has relatively large volume with a low value of gain. There are two resonance frequencies for two switching configuration. In comparison to the afore-mentioned examples, our design has the minimum volume with a very good value of peak gain by simply using AMC surface while simultaneously providing re-configurability. Using the same AMC surface, two switching operations are performed, which in return, generate two resonance frequencies with much better impedance width.

Table 3 shows the performance analysis of the prototype. When all switches are OFF the prototype has a good simulated and measured value for 5G applications. Thus, the design operates at 3.5GHz and 4.2GHz with the help of ideal switches (micro-strip slabs) placed between the two unit cells. In OFF state at low frequency, the value of gain and efficiencies are relatively higher. Similarly in ON state, due to metallic nature of the AMC surface the value of the efficiencies and gain has slightly reduced but still they are good enough to establishment the communication between uplink and down link. The design is fabricated for measuring the simulated results. Figure 12 and Fig. 13 give complete detail of the fabricated design.

VI. CONCLUSION

We presented a novel miniaturized frequency reconfigurable DRA design. In the proposed design, we achieved miniaturization with the help of AMC surface containing nine AMC unit cells. Using the ideal switches between the same AMC surface, the design is reconfigured to another wireless application. For both the switching configuration, the design has a stable radiation

pattern with good value of the realized gain. Also for both the operating frequencies, the prototype has good values of efficiencies as observed through the measurements reported. Thus the proposed design is good enough for real time mentioned applications.

REFERENCES

[1] M. S. Alam, N. Misran, B. Yatib, and M. T. Islam, "Development of electromagnetic band gap structures in the perspective of microstrip antenna design," *Int. J. Antenna Propag.*, p. 22, 2013.

[2] Y. M. Pan, P. F. Hu, X. Y. Zhang, and S. Y. Zheng, "A lowprofile high-gain and wideband filtering antenna with metasurface*," IEEE Trans. Antennas Propag.*, vol. 64, no. 5, pp. 2010-2016, May 2016.

[3] Z. N. Chen, "Bandwidth enhancement of a single-feed circularly polarized antenna using a meta-surface," *IEEE Antennas Propag. Mag.*, vol. 50, no. 2, pp. 39-46, Apr. 2016.

[4] H. Gromath and R. Otin, "Specific absorption rate computations with a nodal-based finite element formulation," *Prog. Electromagn. Res.*, vol. 128, pp. 399-418, 2012.

[5] F. Costa, A. Monorichio, S. Talaricos, and F. M. Valeri, "An active highimpedance surface for low-profile tunable and steerable antennas," *IEEE Antenna Wirel. Propag. Lett.*, vol. 676-680, p. 7, 2008.

[6] R. Dewan, M. K. A. Rahim, I. M. Hamid, M. R. Hamid, H. A. Majid, and M. E. Jalil, "Multiband frequency-reconfigurable antenna using meta-material structure of electromagnetic band gap," *Appl. Phys. A*, vol. 16, p. 123, 2016.

[7] J. Dong, S. Wang, and G. Hu, "Design of recon-figurable ultrawide band antenna with switchable single/dual/triple band notch functions," *Applied Computational Electromagnetics Society Journal*, vol. 34, no. 1, Jan. 2019.

[8] N. A. Al-Shalaby and S. M. Gaber, "Design of dielectric resonator band stop/band pass filters," *Applied Computational Electromagnetics Society Journal*, vol. 34, no. 8, Aug. 2019.

[9] T. Apperley and M. Okoniewski, "An air-gap-based frequency switching method for the dielectric resonator antenna," *IEEE Antennas Wireless Propag. Lett.*, vol. 13, pp. 455-458, 2014.

[10] S. Danesh, M. K. A. Rahim, M. Hamidi, M. R. Hamid, and J. Majid, "Frequency reconfigurable rectangular dielectric resonator antenna," *IEEE Antennas Wireless Propag. Lett.*, vol. 12, pp. 1331-1334, 2013.

[11] S. Dhar, K. Patra, R. Ghatak, B. Gupta, and D. R. Poddar, "Reconfigurable dielectric resonator antenna with multiple polarisation states," *Antennas Propag.*, vol. 12, no. 6, pp. 895-902, 2018.

[12] B.-J. Liu, J.-H. Qiu, S.-C. Lan, and G.-Q. Li, "A wideband-to-narrowband rectangular dielectric resonator antenna integrated with tunable bandpass filter," *IEEE Access*, vol. 7, 2019.

[13] S. Danesh, S. K. A. Rahim, and M. Khalily, "A wideband trapezoidal dielectric resonator antenna with circular polarization," *Progress in Electromagnetics Research L*, vol. 34, pp. 91-100, 2012.

Shahid Khan was born in Landikotal, Pakistan in 1986. He received the B.S. degree in Communication Engineering from the University of Engineering and Technology Peshawar Pakistan and M.S. degree in Satellite Navigation and Related Applications from Politecnico de Torino Italy in 2011. Currently he is doing his Ph.D. from University de Lorraine France. He is working on the Development of Reconfigurable Dielectric Resonator antenna for different wireless applications. Before joining University de Lorraine he worked as a Lecturer in Comsats University Abbottabad from 2012 to 2017.

Hazrat Ali received his B.Sc. and M.Sc. degrees in Electrical Engineering in 2009 and 2012 respectively. He did his Ph.D. in 2015 from University of Science and Technology Beijing, China. He is currently Assistant Professor at Department of Electrical and Computer Engineering, COMSATS University Islamabad, Abbottabad Campus. At CUI, he is the member of the signal processing and machine learning research group. He is also the Course Head for Digital Signal Processing course. His research interests lie in unsupervised learning, generative and discriminative approaches, and speech and medical image processing. He is Associate Editor at IEEE and served as Reviewer at IEEE Access, IEEE Transactions on Neural Networks and Learning Systems, IEEE Transactions on Emerging Topics in Computational Intelligence.

Syed Usman Ali Shah did his bachelor in Telecommunication and Networks from Hazara University Pakistan. He did his Masters from Comsats University Islamabad, Abbotabad Campus in 2017. His has worked on a number of project including microstrip patch antennas, dielectric resonator antennas, reconfigurable antennas.

Haider Ali was born in 1984. He completed his B.S. degree in Telecom Engineering from NUCES, Pakistan, in 2007. He received his Doctorate and a M.S. degree in Electronics Engineering from Politecnico Di Torino, Italy, in 2010, and completed his Ph.D. in Electronics & Communication Engineering from there in 2014. He is currently working as Assistant Professor at the Department of Electrical Engineering, and Technology, University of Technology, Nowshera, Pakistan. His research interests include data acquisition systems, renewable energy materials, power electronics systems, design and development of antenna, radio frequency (RF) front end and telecommunication subsystem for small satellites.

Tanougast Camel was born on May 10, 1972 in Thionville – France. He did his Ph.D. degree from Laboratory LIEN - Univ. Henri Poincaré Nancy 1 in 2011. His Ph.D. thesis topic was "Methodology for Temporal Partitioning for System on Chip Implementation based Run Time Reconfigurable Technology". Currently he is Head of the ASEC Team (smart embedded and sensor systems). He is also serving as a Full Professor in Institute of Higher Learning in Electronics and Automation, University of Lorraine, France. His research interests are Self-organised system based run time reconfigurable technology, Custom Computing and Embedded Systems for Image/Video and Signal applications using FPGAs, Secure Communications and radio communication, reconfigurable embedded and RF systems for different wireless applications. He has authored and co-authored more than 100 articles and conference papers.